

[https://doi.org/10.52326/jes.utm.2023.30\(2\).02](https://doi.org/10.52326/jes.utm.2023.30(2).02)
UDC 539.3:004.42



APPLICATION OF DISCONTINUOUS SOLUTIONS IN BOUNDARY ELEMENT METHOD FOR THE BENDING PROBLEMS OF KIRCHHOFF PLATES WITH AN ARBITRARY CONTOUR

Sergiu Galborean*, ORCID: 0009-0000-9876-492x

Technical University of Moldova, 168 Ștefan cel Mare Blvd., Chișinău, Republic of Moldova

*Corresponding author: Sergiu Galborean, sergiu.galborean@cms.utm.md

Received: 05. 15. 2023

Accepted: 06.12. 2023

Abstract. The discontinuous solutions represent a new direction for the indirect Boundary Element Method (BEM) in the indirect formulation. Discontinuous solutions represent those functions, which when crossing certain lines, the transverse deflection, the slope angle, the bending moment and the generalized shear force may have jumps. These can be used to solve important problems for which the existing methods do not have solutions or a satisfactory accuracy, such as: plates of arbitrary contour, presence of defects, mixed boundary conditions, contact problems, infinite domains etc. In this paper, we describe the methodology of application and the numerical implementation of discontinuous solutions for the bending problems of plates with an arbitrary contour in the classical theory (Kirchhoff). For this purpose, programming codes were developed in the Matlab language, which allowed to calculate the displacements and efforts in the plate. The obtained results were compared with the Finite Element Method (FEM) for different mesh densities.

Keywords: *Boundary Element Method; discontinuous solution; Green function; Kirchhoff plate.*

Rezumat. Soluțiile discontinue reprezintă o nouă direcție pentru Metoda Elementelor de Frontieră (MEFr) în formularea indirectă. Soluțiile discontinue reprezintă acele funcții, care la traversarea anumitor linii, săgeata, unghiul de rotire, momentul de încovoiere și forța tăietoare generalizată pot căpăta salturri. Acestea pot fi utilizate la rezolvarea unor probleme importante pentru care metodele existente nu au soluții sau o acuratețe satisfăcătoare, precum: plăci de contur arbitrar, prezența defectelor, condiții mixte la limită, probleme de contact, domenii infinite etc. În această lucrare este descrisă metodologia de aplicare și implementare numerică a soluțiilor discontinue la calculul plăcilor de un contur arbitrar în teoria clasică (Kirchhoff). În acest scop, au fost elaborate coduri de programare în limbajul Matlab, care au permis de a calcula deplasările și eforturile în placă. Rezultatele obținute au fost comparate cu Metoda Elementelor Finite (FEM) pentru diferite densități ai rețelei de discretizare.

Cuvinte cheie: *Metoda elementelor de Frontieră; soluții discontinue; funcția Green; placă Kirchhoff.*

1. Introduction

Plates are important elements for different resistance structures. Although computational theory has a history of more than 200 years, until now there are no methods that would solve all types of plate bending problems encountered. Some solutions for rectangular and circular plates are presented in weakly convergent Fourier series, but these cannot be used for all boundary conditions and loading cases. Along with the development of the computational techniques, numerical calculation methods were developed. The most used are: the Finite Element Method (FEM) [1, 2] and the Boundary Element Method (BEM) [3-4].

The Finite Element Method (FEM) has become widely used in recent times. It is commonly acknowledged that the majority of FEM programs do not contain plate finite elements with more than three degrees of freedom in the nodes, that could satisfy all boundary conditions. The process of discretization of the entire surface of the plate into finite elements, it usually leads to: a massive system of linear equations, necessity of big initial data, big volume of computer memory. There are, also, difficulties in solving problems that present: stress concentrations, defects, contact problems, plate-bar connections etc.

In recent years the boundary elements method (BEM) intensively develops. In BEM the discretization is applied only to the edge of the plate. Therefore, the number of nodes and elements is reduced compared to FEM, and this also implies the reduction of the system of linear equations by one unit. In BEM we have numerical solution only at the edge of the plate, while in the interior the solutions are analytical and provide more accurate results. In the theory of plates and shells there are two approaches to obtain the integral equations: direct [5, 6] and indirect [7, 8].

For the indirect BEM is offered a new approach which is based on discontinuous solutions. These solutions were obtained by Prof. Moraru Gheorghe [9, 10] for an infinite domain by applying the generalized Fourier transform to the differential equation of plates. Using them as Green Functions [11-13] of influence we can solve a variety of plate bending problems.

2. Materials and Methods

2.1. Governing equation in Kirchhoff plate theory

The differential equation of the deformed median surface of the plate has the form:

$$\Delta\Delta w = \frac{p(x,y)}{D}, \quad (1)$$

where Δ is the Laplace operator, p is the the external load distributed on area;

$D = Eh^3/12(1 - \nu^2)$ is the flexural rigidity, E and ν are Young's modulus and Poisson's ratio.

This differential equation allows to satisfy two boundary conditions for each side.

2.2. Discontinuous solutions for an infinite plate

Consider that in an infinite plate on the axis y ($x = 0$) (Figure 1) there is a defect (crack, plastic hinge, rigid inclusion etc.). When passing from one side of the defect $x = -0$ to the other $x = +0$ the deflection w , the slope angle ϑ_x , the bending moment M_x , and the generalized shear force V_x may obtain jumps (Figure 2). In the local system of coordinates (x, y) we introduce the following notation for the jump of functions:

$$\begin{aligned} w(-0, y) - w(+0, y) &= \langle w(y) \rangle; \\ \theta_x(-0, y) - \theta_x(+0, y) &= \langle \theta_x(y) \rangle; \\ M_x(-0, y) - M_x(+0, y) &= \langle M_x(y) \rangle; \\ V_x(-0, y) - V_x(+0, y) &= \langle V_x(y) \rangle. \end{aligned} \quad (2)$$

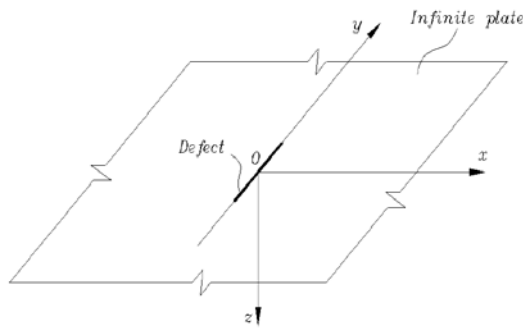


Figure 1. Infinite plate with a defect.

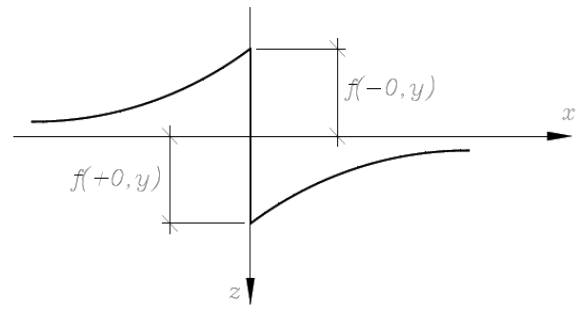


Figure 2. The jump of function f when passing through the defect.

We can obtain the solutions for these jumps by applying the generalized Fourier transform [14] to the differential equation of plates (1), assuming that $q(x, y) = 0$. The relations between concentrated jumps and displacements can be written in the following form:

$$\begin{Bmatrix} \langle w(x, y) \rangle \\ \langle \theta_x(x, y) \rangle \\ \langle \theta_y(x, y) \rangle \end{Bmatrix} = \begin{bmatrix} g_{11} & g_{12} & g_{13} & g_{14} \\ g_{21} & g_{22} & g_{23} & g_{24} \\ g_{31} & g_{32} & g_{33} & g_{34} \end{bmatrix} \begin{Bmatrix} \langle w(y) \rangle \\ \langle \theta_x(y) \rangle \\ \langle M_x(y) \rangle \\ \langle V_x(y) \rangle \end{Bmatrix}, \tag{3}$$

where elements g_{ij} are given [8]:

$$g_{11} = -\frac{1}{4\pi} \frac{x}{r^4} [(3 - \nu)x^2 + (1 + \nu)y^2]; \quad g_{12} = -\frac{1}{4\pi} \left[(1 + \nu) \ln r + (1 - \nu) \frac{x^2}{r^2} \right];$$

The relations between jumps and efforts are given by:

$$\begin{Bmatrix} M_x(x, y) \\ M_y(x, y) \\ M_{xy}(x, y) \\ Q_x(x, y) \\ Q_y(x, y) \end{Bmatrix} = \begin{bmatrix} t_{11} & t_{12} & t_{13} & t_{14} \\ t_{21} & t_{22} & t_{23} & t_{24} \\ t_{31} & t_{32} & t_{33} & t_{34} \\ t_{41} & t_{42} & t_{43} & t_{44} \\ t_{51} & t_{52} & t_{53} & t_{54} \end{bmatrix} \begin{Bmatrix} \langle w(y) \rangle \\ \langle \theta_x(y) \rangle \\ \langle M_x(y) \rangle \\ \langle V_x(y) \rangle \end{Bmatrix}, \tag{4}$$

where elements t_{ij} are given [8]:

$$t_{11} = \frac{3(1 - \nu)^2 D}{2\pi} \frac{x}{r^8} (x^4 - 6x^2y^2 + y^4);$$

$$t_{21} = \frac{(1 - \nu) D}{2\pi} \frac{x}{r^8} [-(5 - \nu)x^4 + 2(11 - 7\nu)x^2y^2 + 3(1 + 3\nu)y^4];$$

The relations between jumps and the generalized shear force [8]:

$$\begin{Bmatrix} \langle V_x(x, y) \rangle \\ \langle V_y(x, y) \rangle \end{Bmatrix} = \begin{bmatrix} l_{11} & l_{12} & l_{13} & l_{14} & l_{15} \\ l_{21} & l_{22} & l_{23} & l_{24} & l_{25} \end{bmatrix} \begin{Bmatrix} \langle w(y) \rangle \\ \langle \theta_x(y) \rangle \\ \langle M_x(y) \rangle \\ \langle V_x(y) \rangle \end{Bmatrix}, \tag{5}$$

where elements l_{ij} are given:

$$l_{11} = \frac{3(1 - \nu) D}{2\pi r^{10}} [(7 - 3\nu)x^6 - 5(11 - 7\nu)x^4y^2 + 5(1 - 5\nu)x^2y^4 + (3 + \nu)y^6];$$

$$l_{12} = -\frac{3(1 - \nu)^2 D}{2\pi} \frac{x}{r^8} (x^4 - 6x^2y^2 + y^4); \quad \dots$$

2.3. The efforts in plates with arbitrary boundary

If we consider the obtained solutions as Green functions of influence [11-13] and applying the principle of superposition we can write the discontinuous solutions for the defect located on an arbitrary contour L (Figure 3).

If we use coordinate transformation from one local system (\bar{x}, \bar{y}) to another local system (n, t) , then we obtain:

$$\begin{aligned} w^*(P) &= \int_L \bar{w}(P, Q) ds_Q; & \theta_n^*(P) &= \int_L [\bar{\theta}_x(P, Q) \cos \gamma + \bar{\theta}_y(P, Q) \sin \gamma] ds_Q; \\ M_n^*(P) &= \int_L [\bar{M}_x(P, Q) \cos^2 \gamma + \bar{M}_y(P, Q) \sin^2 \gamma + 2\bar{M}_{xy}(P, Q) \cos \gamma \sin \gamma] ds_Q; \\ M_{nt}^*(P) &= \int_L \{[\bar{M}_y(P, Q) - \bar{M}_x(P, Q)] \cos \gamma \sin \gamma + M_{xy}(P, Q)(\cos^2 \gamma - \sin^2 \gamma)\} ds_Q; \\ Q_n^*(P) &= \int_L [\bar{Q}_x(P, Q) \cos \gamma + \bar{Q}_y(P, Q) \sin \gamma] ds_Q; & V_n^*(P) &= Q_n^* + \frac{\partial M_{nt}^*}{\partial t}, \end{aligned} \quad (6)$$

where $\gamma = \beta - \alpha$.

The discontinuous solutions can also be applied to solve fundamental plate bending problems. In such cases, the edge is treated as a defect within an infinite plate. As we approach the edge from within the region occupied by the plate, the jumps are assumed to be equal to the values on the boundary. On the other hand, as we approach the edge from outside, these jumps are considered equal to zero.

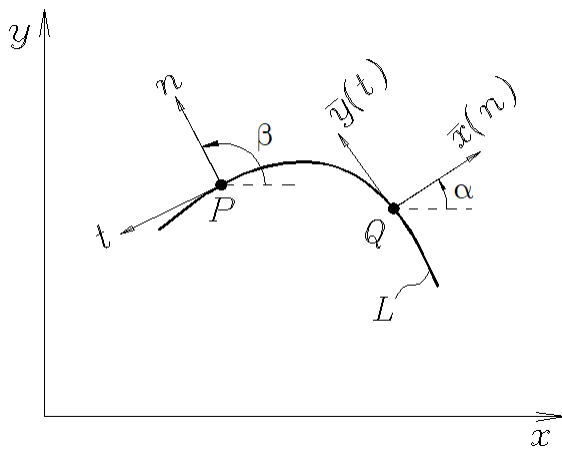


Figure 3. Local systems of coordinates on contour L .

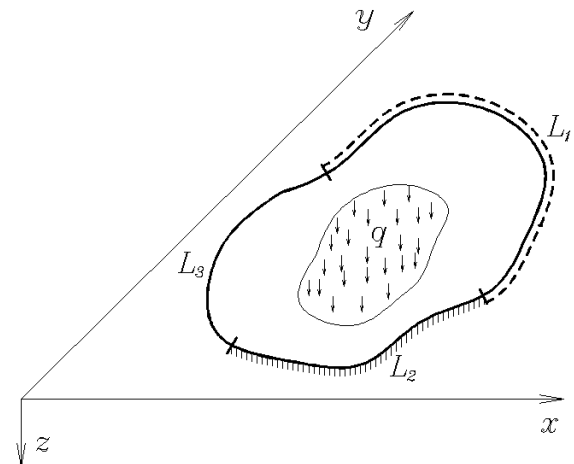


Figure 4. Plate of arbitrary shape.

2.4. Numerical implementation of discontinuous solutions in BEM

Consider a plate of arbitrary shape (Figure 3). On the edge L_1 the plate is simply supported, on L_2 – clamped and on L_3 – free.

To write the boundary integral equations, the deformable state of the plate is expressed as a combination of two states: the first one (marked with an asterisk) corresponds to the concentrated jumps on the line L of the defect, while the second one (marked with a circle) – to the external loads.

The boundary conditions are:

- for simply supported edge (L_1)

$$w^* + w^o = 0; \quad M_n^* + M_n^o = 0; \quad (\langle \theta_n \rangle \neq 0; \quad \langle V_n \rangle \neq 0);$$

- for clamped edge (L_2)

$$\begin{aligned}
 & w^* + w^o = 0; \quad \theta_n^* + \theta_n^o = 0; \quad (\langle M_n \rangle \neq 0; \quad \langle V_n \rangle \neq 0); \\
 - & \text{ for free edge } (L_3) \\
 & M_n^* + M_n^o = 0; \quad V_n^* + V_n^o = 0; \quad (\langle w \rangle \neq 0; \quad \langle \theta_n \rangle \neq 0).
 \end{aligned}$$

For example, if the plate is subjected to a point force F with coordinates a_0, b_0 , the solutions due to the external load have the form:

$$\begin{aligned}
 w_i^o &= F \cdot g_{14}(x_i^m - a_0, y_i^m - b_0); \\
 \theta_{ni}^o &= F(n_x \theta_{xi}^o + n_y \theta_{yi}^o) = F[n_x g_{24}(x_i^m - a_0, y_i^m - b_0) + n_y g_{34}(x_i^m - a_0, y_i^m - b_0)]; \\
 M_{ni}^o &= F(n_x^2 M_{xi}^o + n_y^2 M_{yi}^o + 2n_x n_y M_{xyi}^o) = F[n_x^2 t_{14}(x_i^m - a_0, y_i^m - b_0) + \\
 &+ n_y^2 t_{24}(x_i^m - a_0, y_i^m - b_0) + 2n_x n_y t_{34}(x_i^m - a_0, y_i^m - b_0)]; \\
 V_{ni}^o &= F(n_x V_{xi}^o + n_y V_{yi}^o) = F[n_x l_{14}(x_i^m - a_0, y_i^m - b_0) + n_y l_{24}(x_i^m - a_0, y_i^m - b_0)] \quad (7)
 \end{aligned}$$

where $n_x = \cos \alpha$ and $n_y = \sin \alpha$.

For other loading types the solutions can be obtained by integrating the expressions (7) on the line or on the area of the load distribution.

If we discretize the contour L into a set of constant elements we can obtain the following system of equations:

$$\left. \begin{aligned}
 \sum_{j=n_{L3}} w_{ij}^1 \langle w_j \rangle + \sum_{j=n_{L1}, n_{L3}, n_{Ld}} w_{ij}^2 \langle \theta_{nj} \rangle + \sum_{j=n_{L2}} w_{ij}^3 \langle M_{nj} \rangle + \sum_{j=n_{L1}, n_{L2}} w_{ij}^4 \langle V_{nj} \rangle &= -w_i^o; \quad (i = n_{L1}, n_{L2}) \\
 \sum_{j=n_{L3}} \theta_{ij}^1 \langle w_j \rangle + \sum_{j=n_{L1}, n_{L3}, n_{Ld}} \theta_{ij}^2 \langle \theta_{nj} \rangle + \sum_{j=n_{L2}} \theta_{ij}^3 \langle M_{nj} \rangle + \sum_{j=n_{L1}, n_{L2}} \theta_{ij}^4 \langle V_{nj} \rangle &= -\theta_{ni}^o; \quad (i = n_{L2}) \\
 \sum_{j=n_{L3}} m_{ij}^1 \langle w_j \rangle + \sum_{j=n_{L1}, n_{L3}, n_{Ld}} m_{ij}^2 \langle \theta_{nj} \rangle + \sum_{j=n_{L2}} m_{ij}^3 \langle M_{nj} \rangle + \sum_{j=n_{L1}, n_{L2}} m_{ij}^4 \langle V_{nj} \rangle &= -M_{ni}^o; \quad (i = n_{L1}, n_{L3}, n_{Ld}) \\
 \sum_{j=n_{L3}} v_{ij}^1 \langle w_j \rangle + \sum_{j=n_{L1}, n_{L3}, n_{Ld}} v_{ij}^2 \langle \theta_{nj} \rangle + \sum_{j=n_{L2}} v_{ij}^3 \langle M_{nj} \rangle + \sum_{j=n_{L1}, n_{L2}} v_{ij}^4 \langle V_{nj} \rangle &= -V_{ni}^o; \quad (i = n_{L3})
 \end{aligned} \right\} (8)$$

where: n_{L1}, n_{L2}, n_{L3} – the index number of the boundary elements on the edge: L_1, L_2 and L_3 , respectively.

By solving the system of equations (8) all the jumps on the boundary will be known, so that the displacements and the efforts in any point inside the plate can be calculated, these being expressed by the obtained jumps. For example, if it is necessary to calculate the displacement at any point k from the interior of the plate (Figure 5), the expression take the form:

$$w_k = \sum_{j=n_{L3}} g_{11} \langle w_j \rangle + \sum_{j=n_{L1}, n_{L3}, n_{Ld}} g_{12} \langle \theta_{nj} \rangle + \sum_{j=n_{L2}} g_{13} \langle M_{nj} \rangle + \sum_{j=n_{L1}, n_{L2}} g_{14} \langle V_{nj} \rangle + w_k^o. \quad (9)$$

The bending moment at the point k , acting in direction d (Figure 5):

$$\begin{aligned}
 M_k^d &= \sum_{j=n_{L3}} (c^2 t_{11} + s^2 t_{21} + 2cs t_{31}) \langle w_j \rangle + \sum_{j=n_{L1}, n_{L3}, n_{Ld}} (c^2 t_{12} + s^2 t_{22} + 2cs t_{32}) \langle \theta_{nj} \rangle + \\
 &+ \sum_{j=n_{L2}} (c^2 t_{13} + s^2 t_{23} + 2cs t_{33}) \langle M_{nj} \rangle + \sum_{j=n_{L1}, n_{L2}} (c^2 t_{14} + s^2 t_{24} + 2cs t_{34}) \langle V_{nj} \rangle + \\
 &n_x^2 M_{x,k}^o + n_y^2 M_{y,k}^o + 2n_x n_y M_{xy,k}^o. \quad (10)
 \end{aligned}$$

The terms $g_{11}, g_{12}, \dots, t_{54}$ from relations (9) and (10) will be calculated using the solutions from (3) and (4) substituting: x_i with x_k and y_i with y_k .

Where: x_k and y_k represent the coordinates of point k in the global system;

$c = \cos(\beta_k - \alpha_j)$; $s = \sin(\beta_k - \alpha_j)$; $n_x = \cos(\beta_k)$; $n_y = \sin(\beta_k)$;

$w_k^o, M_{x,k}^o, M_{y,k}^o, M_{xy,k}^o$ represent the solutions at the point k due to the external loads. For example, in case of a point force these solutions can be obtained from (7) substituting x_i^m with x_k and y_i^m with y_k . For other loading types – by integrating the expressions (7) on the line or on the area of the load distribution.

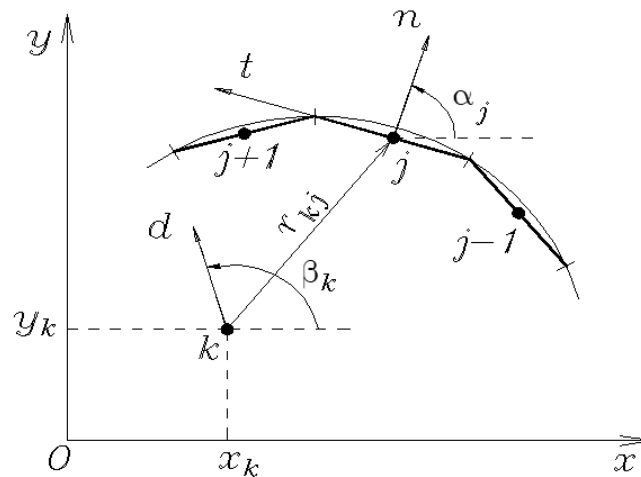


Figure 5. The position of the interior point k relative to the constant boundary elements.

In the same manner, at any point, we can calculate the expressions for slope angles and shear forces. For BEM analysis based on discontinuous solutions we developed a computational program DISSOL using Matlab programming language and sources from specialized literature [15, 16], that allowed us to calculate the deflections and stresses in every point of the plate.

3. Results and Discussion

We propose to examine a plate of an arbitrary contour having one part of the contour simply supported and the another – clamped. Two loading cases are proposed: first – point force loading (Figure 6, a); second – uniform load distributed on a rectangular area (Figure 6, b).

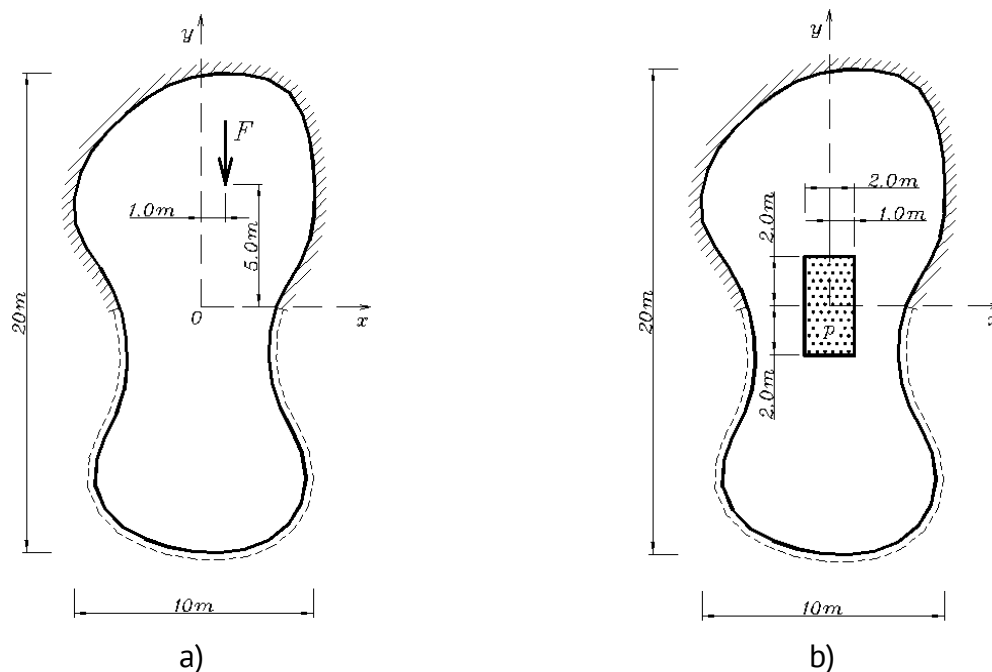


Figure 6. Plate of arbitrary contour loaded with: a) point force; b) area load.

For plates with an arbitrarily complicated contour, which cannot be described by a mathematical equation, analytical solutions cannot be found in the specialized literature. This type of problem can only be solved by numerical methods such as FEM [1, 2] or BEM [3, 4]. The most popular is FEM, but, as is well known, the accuracy of this method depends a lot on the

mesh density and the types of finite elements used (triangular, rectangular, trapezoidal, etc.). Another alternative would be the use of BEM based on discontinuous solutions, described in this paper and in other works [9, 10, 17].

In order to validate and demonstrate the efficiency of the proposed method, we will analyze a plate with an arbitrary contour by building BEM models (with the application of discontinuous solutions) and FEM models, and we will compare the results obtained by both numerical methods.

For BEM model we used the previously mentioned program (DISSOL) to calculate the deflections and stresses in every point of the plate. For this purpose, the contour of the plate was discretized into 50 constant boundary elements (Figure 7, a).

For FEM analysis we built 3 models: i) 165 elements and 182 nodes (Figure 7, b); ii) 321 elements and 320 nodes (Figure 7, c); iii) 641 elements and 663 nodes (Figure 7, d).

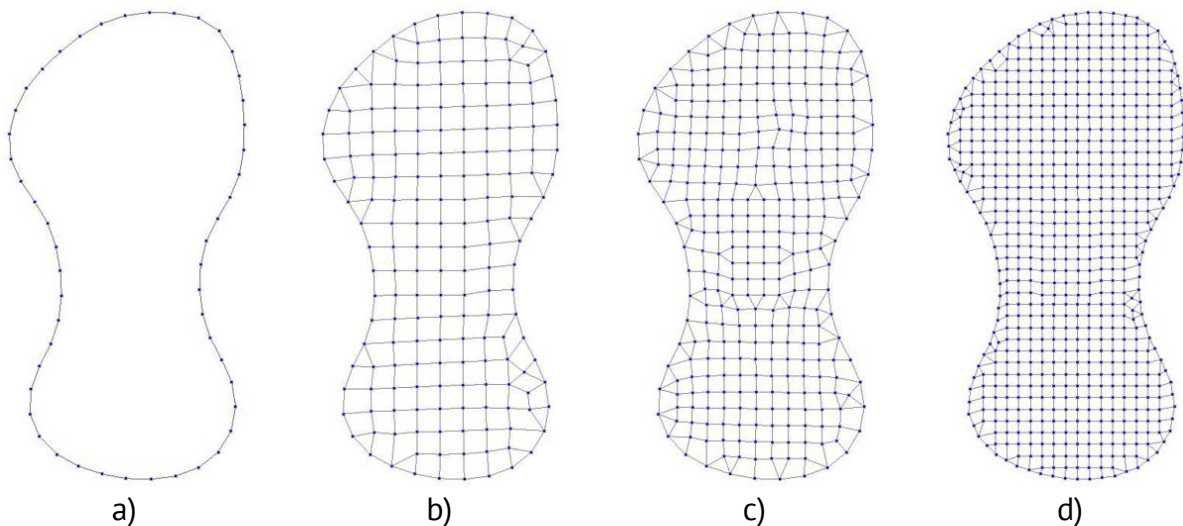
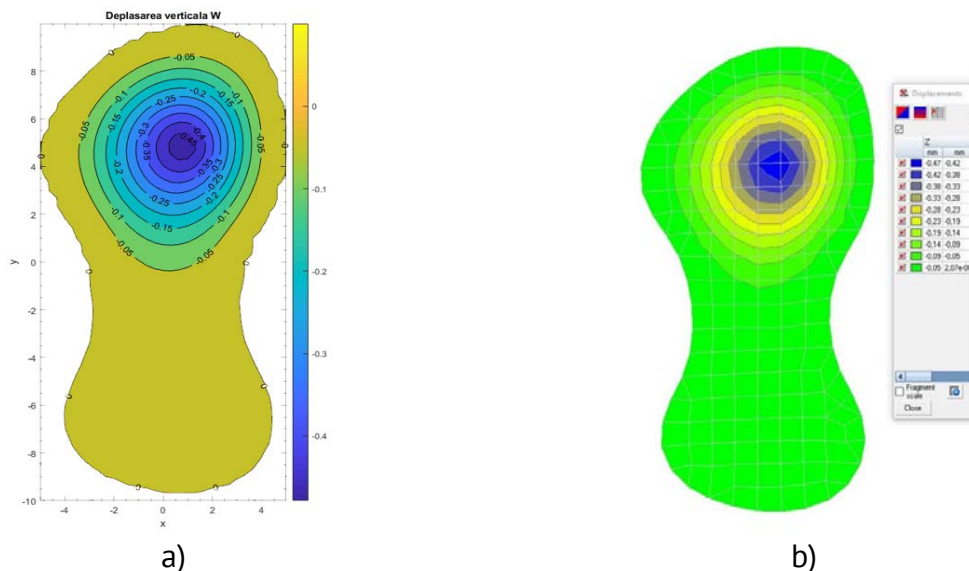


Figure 7. Plate models: a) BEM – 50 elem.; b) FEM – 165 elem. (182 nodes); c) FEM – 321 elem. (320 nodes); d) FEM – 641 elem. (663 nodes).

Case 1. We obtained the deflection field due to a point force DISSOL (Figure 8, a) and also, using a FEM program (SCAD Office) for 3 models of mesh discretization (Figure 8, b, c, d).

The obtained results were introduced in the table below. It contains the maximal values of deflection and the deviations of the results in FEM models compared to BEM model.



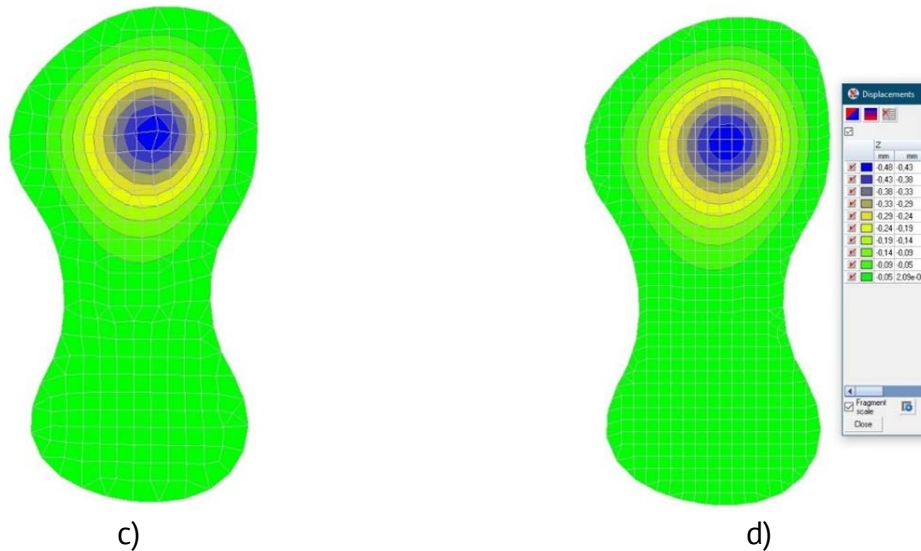


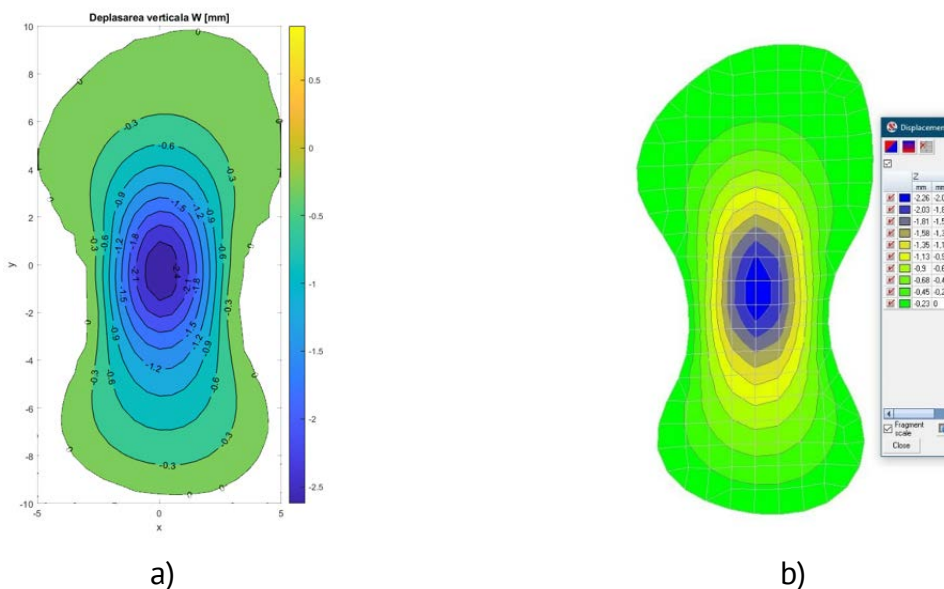
Figure 8. Deflection field due to a point force: a) BEM – 50 elem.; b) FEM – 165 elem.; c) FEM – 321 elem.; d) FEM – 641 elem.

Table 1

The maximal deflection W_{max} due to a point force applied on a plate with arbitrary contour

Numerical method	Nr. of elements	Dimension of the global matrix	Max. deflection W_{max} [mm]	Deviations compared to BEM model [%]
BEM	50	100	0.4783	-
FEM (i)	165	840	0.4702	1.69
FEM (ii)	321	1668	0.4738	0.94
FEM (iii)	641	3476	0.4767	0.33

Case 2. We obtained the deflection field due to a uniform load distributed on a square area using the developed Matlab codes (Figure 9, a) and also, using a FEM program (SCAD Office) for 3 models of mesh discretization (Figure 9, b, c, d).



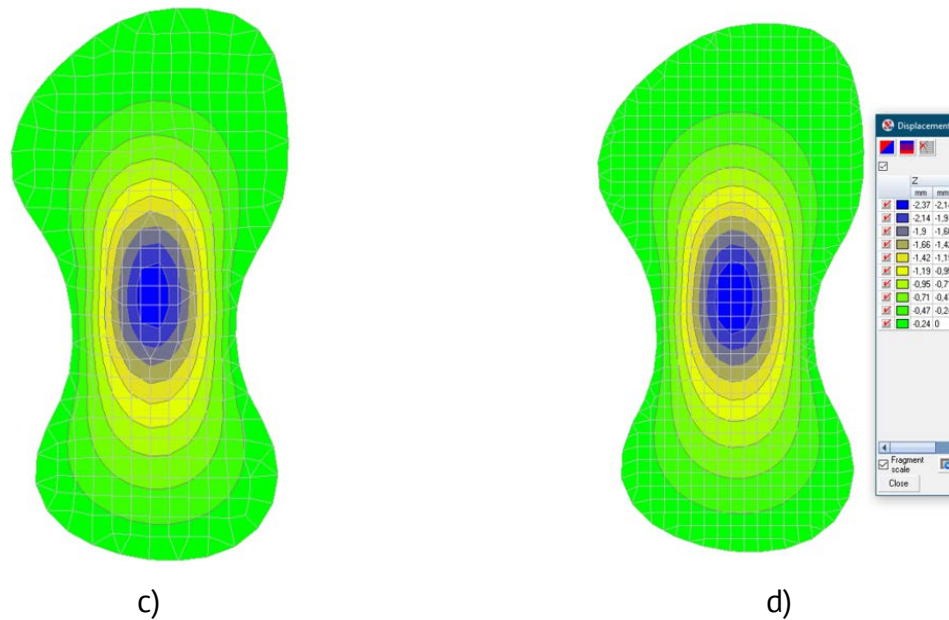


Figure 9. Deflection field due to a uniform load distributed on a square area: a) BEM – 50 elem.; b) FEM – 165 elem.; c) FEM – 321 elem.; d) FEM – 641 elem.

The obtained results were introduced in the table below. It contains the maximal values of deflection and the deviations of the results in FEM models compared to BEM model.

Analyzing the obtained results illustrated in Figure 8 and Figure 9, we observe that for the FEM models with a relatively reduced number of elements, the deflection curves, especially in the areas of load action, show some polygonal shapes, and for the FEM models with denser mesh, the deflection curves become more regularized, acquiring more curvilinear shapes and the results approach those obtained in BEM models [18].

Table 2

The maximal deflection W_{max} due to a distributed load

Numerical method	Nr. of elements	Dimension of the global matrix	Max. deflection W_{max} [mm]	Deviations compared to BEM model [%]
BEM	50	100	2.520	-
FEM (i)	165	840	2.258	10.0
FEM (ii)	321	1668	2.300	8.70
FEM (iii)	641	3476	2.375	5.75

As we can observe in Table 2, for the second case of loading distributed on a rectangular area, to obtain an acceptable precision FEM models require solving a massive system of linear equations (3476 eq.), tens of times larger than BEM models (100 eq.). Also, in the discretization process of the curvilinear contour, the problem of geometry approximation appears, which involves the use of irregular elements (triangular, quadrilateral, etc.) for the mesh, that can affect the accuracy of the results in the neighboring elements. In BEM due to the fact that the solutions at the edge are described numerically, and in the interior – analytically, this influence has a local effect present only at the edge of the plate and does not spread in interior. The problem of approximating the curvilinear

contour can be improved using higher-order boundary elements (linear, quadratic, cubic etc.). We mention that in the BEM models presented in this paper, constant boundary elements of the lowest precision were used, which still provide results quite close to the analytical ones [17].

4. Conclusions

The Boundary Element Method based on discontinuous solutions, described in this paper, represents a new direction in the solid mechanic. These solutions were applied to the calculation of a plate with an arbitrary contour, different modes of support and loads. The obtained results were compared to FEM, demonstrating a good accuracy and applicability.

One of the main advantages of the BEM is that the discretization is applied only to the edge of the plate reducing the size of the system of linear equations by one unit and leading to a minimal use of computer resources. The numerical implementation of the proposed method offered us the possibility to develop Matlab codes for solving practical problems, which cannot be solved using analytical methods.

Acknowledgments: This paper is dedicated to the memory of Prof. Gheorghe Moraru, my first scientific coordinator for my doctoral thesis.

Special thanks to my wife Tatiana Galbinean who helped me translate and edit the text.

Conflicts of Interest: The authors declare no conflict of interest.

References

1. Moraru, G.A. *Introducere în metoda elementelor finite și de frontieră*. UTM, Chisinau, 2002, 176 p.
2. Zienkiewicz, O.C. *The Finite Element Method in Engineering Science*. McGraw-Hill, London, UK, 1971, 521 p.
3. Brebbia, C.A.; Walker, S. *Boundary Element Techniques in Engineering*. Butterworths, London, UK, 1980, 220 p.
4. Katsikadelis, J.T. *Boundary Elements. Theory and Applications*. Elsevier, UK, 2002, 448 p.
5. Jaswon, M.A.; Maiti, M. An integral equations formulation of plate bending problems. *J. Engng Math* 1968, 2, pp. 83-93.
6. Rizzo, F.J. An integral equation approach to boundary value problem of classical elastostatics. *Q. Appl. Math.* 1967, 25, pp. 83-95.
7. Ventsel, E. An indirect boundary element method for plate bending analysis. *Int. J. Numer. Meth. Engng.* 1997, 40, pp. 1597-1610.
8. Muskhelishvili, N.I. *Singular Integral Equations: Boundary Problems of Function Theory and Their Applications to Mathematical Physics*. Dover Publications, New York, SUA, 2011, 464 p.
9. Moraru, G.A. *Discontinuous solutions in the statics of deformable bodies*. Tehnica-Info, Chisinau, 2015, 398 p.
10. Moraru, G.A. BEM based on discontinuous solutions in the theory of Kirchhoff plates on an elastic foundation. *Eng. Anal. Bound. Elem.* 2006, 30, pp. 382-390.
11. Sheremet, V.D. *Handbook of Greens Functions and Matrices*. WIT Press, Southampton, UK, 2003, 304 p.
12. Melnikov, Y.A. *Influence Functions and Matrices*. Marcell Dekker, New York, SUA, 1998, 488 p.
13. Duffy, D.G. *Green's Functions with Applications*. 2nd Edition, Chapman & Hall/CRC, New York, SUA, 2015, 685 p.
14. Sneddon, I.N. *Fourier Transforms*. McGraw-Hill Book Co, New York, SUA, 1951, 560 p.
15. Beer, C.; Smith, I.; Duenser, C. *The Boundary Element Method with Programming for Engineers and Scientists*. Springer, Viena, Austria, 2010, 512 p.
16. Pozrikidis, C.A. *Practical Guide to Boundary Element Methods with the Software Library BEMLIB*. CRC Press, Boca Raton, SUA, 2002, 440 p.
17. Galbinean, S.G. Soluții discontinue pentru calculul plăcilor în teoria clasică. *Akademios* 2018, 1, pp. 31-35.
18. Galbinean, S.G. Calculation errors of the plates using finite element method. *Meridian Ingineresc* 2013, 2, pp. 64-66.

Citation: Galbinean, S. Application of discontinuous solutions in boundary element method for the bending problems of Kirchhoff plates with an arbitrary contour. *Journal of Engineering Science* 2023, 30 (2), pp. 23-33. [https://doi.org/10.52326/jes.utm.2023.30\(2\).02](https://doi.org/10.52326/jes.utm.2023.30(2).02).

Publisher's Note: JES stays neutral with regard to jurisdictional claims in published maps and institutional affiliations.



Copyright:© 2023 by the authors. Submitted for possible open access publication under the terms and conditions of the Creative Commons Attribution (CC BY) license (<https://creativecommons.org/licenses/by/4.0/>).

Submission of manuscripts:

jes@meridian.utm.md